10-1-2005

argE-Encoded N-Acetyl-l-Ornithine Deacetylase from *Escherichia coli* Contains a Dinuclear Metalloactive Site

Wade C. McGregor
Utah State University

Sabina I. Swierczek
Utah State University

Brian Bennett
Marquette University, brian.bennett@marquette.edu

Richard C. Holz
Marquette University, richard.holz@marquette.edu

argE-Encoded *N*-Acetyl-l-Ornithine Deacetylase from *Escherichia coli* Contains a Dinuclear Metalloactive Site

Wade C. McGregor

Department of Chemistry and Biochemistry,
Utah State University,
Logan, UT

Sabina I. Swierczek

Department of Chemistry and Biochemistry,
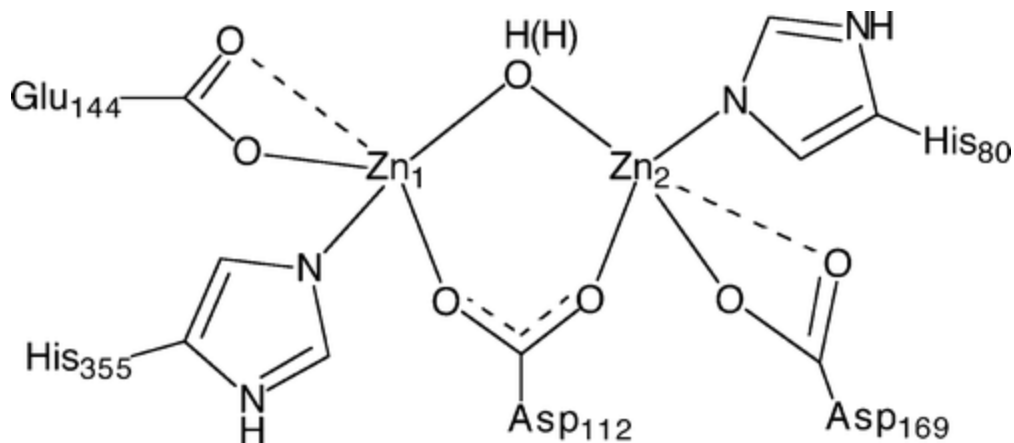*Utah State University,*
Logan, UT

Brian Bennett

National Biomedical EPR Center, Department of Biophysics,
Medical College of Wisconsin,
Milwaukee, WI

Richard C. Holz

Department of Chemistry and Biochemistry,
Utah State University,
Logan, UT

Abstract

The catalytic and structural properties of the *argE*-encoded *N*-acetyl-l-ornithine deacetylase (ArgE) from *Escherichia coli* were investigated. On the basis of kinetic and ITC (isothermal titration calorimetry) data, Zn(II) binds to ArgE with K_d values that differ by ~20 times. Moreover, ArgE exhibits ~90% of its full catalytic activity upon addition of one metal ion. Therefore, ArgE behaves similarly to the aminopeptidase from *Aeromonas proteolytica* (AAP) in that one metal ion is the catalytic metal ion while the second likely plays a structural role. The *N*-acetyl-l-ornithine (NAO) deacetylase activity of ArgE showed a linear temperature dependence from 20 to 45 °C, indicating that the rate-limiting step does not change over this temperature range. The activation energy for NAO hydrolysis by ArgE was 25.6 kJ/mol when loaded with Zn(II) and 34.3 kJ/mol when loaded with Co(II). Electronic absorption and EPR (electron paramagnetic resonance) spectra of [Co·(ArgE)] and [CoCo(ArgE)] indicate that both divalent metal binding sites are five coordinate. In addition, EPR data show clear evidence of spin−spin coupling between the Co(II) ions in the active site but only after addition of a second equivalent of Co(II). Combination of these data provides the first physical evidence that the ArgE from *E. coli* contains a dinuclear Zn(II) active site, similar to AAP and the carboxypeptidase G_2 from *Pseudomonas sp*. strain RS-16 (CPG2).

Pathogenic bacterial infections are a significant and growing medical problem in the United States and throughout the world.[1-3] According to recent estimates from the United States Centers for Disease Control and Prevention (the CDC), more than 10 million people died worldwide from bacterial infections in 1995,[4] in part because an increasing number of disease-causing microbes have become resistant to antibiotics.[5-8] Tuberculosis, staph, malaria, and childhood meningitis are just a few of the diseases that have become hard to treat with available antibiotics.[7,9] For instance, the number of *Staphylococcus aureus* strains, resistant to even the most powerful

drugs such as vancomycin, is increasing by ~8% per year.[2] An important aspect of this problem is the resiliency of bacteria and other microorganisms that causes resistance to develop against antibiotics.[7,8] Even a single random gene mutation can have a large impact on an antibiotic's ability to kill that microorganism. Microbes commonly acquire genes, including those encoding for resistance, by direct transfer from members of their own species or from unrelated microbes. This problem has been amplified because bacteria have been exposed to the same two general classes of antibiotics for roughly 30 years.[1] Therefore, resistance to such compounds evolves rapidly, typically within a decade of a drug's release to market. Since many of the broad-spectrum antibiotics contain β-lactam functional units that target enzymes involved in bacterial cell wall synthesis or pathways involved in cell replication,[7,9] new enzymatic targets must be located so novel inhibitors can be synthesized, providing a new class of antibiotic.

N-Acetyl-l-ornithine deacetylases (ArgEs) are a group of bacterial isozymes that can potentially function as a new enzymatic target for a novel set of antibiotics.[10,11] Prokaryotes synthesize arginine through a series of eight enzymatically catalyzed reactions that differ from those of eukaryotes by two key steps: (i) acetylation of glutamate and (ii) the subsequent deacetylation of the arginine precursor *N*-acetyl-l-ornithine (NAO) by ArgE. Because ornithine is required not only for the synthesis of arginine in bacteria, but also for polyamines involved in DNA replication and cell division, NAO deacetylation is critical for bacterial proliferation. Indeed, when Meinnel and co-workers transformed an arginine auxotrophic bacterial strain void of NAO deacetylase activity with a plasmid containing *argE*, an Arg$^+$ phenotype resulted.[10] However, when the start codon (ATG) of *argE* in the same plasmid was changed to the Amber codon (TAG), the resultant plasmid was unable to relieve arginine auxotrophy in the same cell strain. Therefore, ArgE is required for cell viability, making ArgE a potential target for a new class of antibiotics.

Sequence alignment of several ArgE genes with those of the crystallographically characterized aminopeptidase from *Aeromonas proteolytica* (AAP) and the carboxypeptidase G$_2$ from *Pseudomonas sp*. strain RS-16 (CPG$_2$), indicated that all of the amino acids that function

as metal ligands in AAP and CPG_2 are strictly conserved in ArgEs.[11] The X-ray crystal structures of both CPG_2 and AAP reveal a (μ-aquo)(μ-carboxylato)dizinc(II) active site with one terminal carboxylate and histidine residue bound to each metal ion.[12,13] Both Zn(II) ions in AAP and CPG_2 reside in a distorted tetrahedral or trigonal bipyramidal coordination geometry, with a Zn−Zn distance of 3.5 and 3.3 Å for AAP and CPG_2, respectively.[12,13] Therefore, ArgE enzymes have been proposed to contain dinuclear Zn(II) active sites; however, no spectroscopic or structural data of any kind are available for ArgE enzymes, so the active site structure is unknown. To determine if ArgE does in fact contain a dinuclear Zn(II) active site, we examined the Zn(II)- and Co(II)-loaded ArgE enzyme from *E. coli* using both kinetic and spectroscopic methods. These data indicate that ArgE enzymes do in fact contain a dinuclear metalloactive site, information that is critical for the design of novel small molecule inhibitors that have the potential to function as a new class of antibiotic.

Materials and Methods

Enzyme Expression and Purification. All chemicals used in this study were purchased from commercial sources and of the highest quality available. The recombinant ArgE from *E. coli* was expressed and purified, as previously described with minor modifications, from a stock culture kindly provided by Professor John Blanchard.[11] Briefly, ArgE was purified from *E. coli* BL21 (DE3) cells hosting the pET-27a(+)*argE* overexpression construct. A 100 mL solution of Leuria Bertani (LB) broth containing 100 μg/mL of ampicillin was inoculated with the ArgE expression cell line and shaken for ~7 h at 225 rpm at 37 °C and was used to inoculate 10 L of LB medium containing 100 μg/mL ampicillin. Cells were grown at 37 °C to an optical density of ~1.2 at 600 nm, cooled to 18 °C, and induced with 2.4 g (1 mM) isopropyl-β-d-thiogalactopyranoside (IPTG). After 3 h cells were harvested by centrifugation at 8000 rpm for 15 min, resuspended in 40 mL of 10 mM Tricine (*N*-tris[hydroxymethyl]methylglycine) buffer, pH 7.5, containing 1 mM phenyl methyl sulfonyl fluoride (PMSF), 10 mg of lysozyme, and 5 mg of DNase I and stirred for 30 min. The cells were then lysed by four 1-min rounds of sonication (Heat systems-Ultrasonics, Inc.) separated by 1-min incubations on ice. The cell debris was removed by centrifugation at 18 000 rpm for 45 min. The

supernatant was then concentrated to less than 10 mL in a 180 mL Amicon stirred-cell concentrator with a YM-10 membrane and loaded onto a fast-flow Q-Sepharose column (Amersham Pharmacia Biotech) that had been equilibrated with 10 mM Tricine buffer pH 7.5. A 0.0−0.3 M linear gradient of NaCl was used with a flow rate of 4.0 mL/min for 420 min, and ArgE eluted from the column at 0.25−0.30 M NaCl. These fractions were combined and concentrated in an Amicon stirred-cell concentrator to less than 10 mL. One molar NaCl was added to the concentrated protein, which was then loaded onto an Octyl-Sepharose (Amersham Pharmacia Biotech) column that had been equilibrated with 10 mM Tricine buffer, pH 7.5, containing 1 M NaCl. The column was washed with several volumes of this high-salt buffer at a rate of 4 mL/min, and several contaminating proteins eluted. Subsequently, the elution buffer was changed to 10 mM Tricine, pH 7.5, without NaCl, which eluted ArgE from the column. The resultant ArgE enzyme was >98% homogeneous by SDS-gel electrophoresis, concentrated to ~1 mM, and stored at 4 °C.

Preparation of Apo-ArgE. ArgE was dialyzed for 48 h at 4 °C against 20 mM Na_2EDTA in 50 mM HEPES (4-(2-hydroxyethyl)-1-piperazineethanesulfonic acid) buffer, pH 7.5, and then exhaustively dialyzed against Chelex 100 treated HEPES buffer. ArgE was inactive and found to contain no detectable metals ions via inductively coupled plasma-atomic emission spectrometry (ICP-AES). Metal insertion was effected by direct addition of a solution of $CoCl_2$ (99.999%; Strem Chemicals) under anaerobic conditions in a Coy soft-sided glovebox (Ar/5% H_2, ≤ 1 ppm O_2; Coy Laboratories) followed by a 30 min incubation period at 20−25 °C. Excess Co(II) was removed by successive dilution and concentration of [Co•(ArgE)] or [CoCo(ArgE)] in an Amicon Centricon-10 micro-concentrator under anaerobic conditions.

Enzymatic Assay of ArgE. ArgE activity was measured by the method of Javid-Majd and Blanchard.[11] In this assay the hydrolysis of 2 mM *N*-acetyl-l-ornithine (NAO) (50 mM Chelex 100 treated K_2HPO_4, pH 7.5) was measured spectrophotometrically at 25 °C by monitoring the peptide bond cleavage forming acetate and l-ornithine. The extent of hydrolysis was calculated by monitoring the decrease in absorbance at 214 nm ($\Delta\varepsilon_{214} = 103$ M^{-1} cm^{-1}). The specific activity of purified ArgE

with NAO was typically found to be 2000 units per milligram of enzyme. One unit was defined as the amount of enzyme that releases 1 µmol of ornithine at 25 °C in 60 s. Catalytic activities were determined within ±10% error. Initial rates were fit directly to the Michaelis−Menten equation to obtain the catalytic constants K_m and k_{cat}.

Isothermal Titration Calorimetry. Isothermal titration calorimetry (ITC) measurements were carried out on a MicroCal OMEGA ultrasensitive titration calorimeter. The divalent metal ion titrants and apo-enzyme solutions were prepared in Chelex 100 treated 25 mM HEPES buffer at pH 7.5. Stock buffer solutions were thoroughly degassed before each titration. The enzyme solution (60−90 µM) was placed in the calorimeter cell and stirred at 200 rpm to ensure rapid mixing. Typically, 4−6 µL of titrant was delivered over 7.6 s with a 6 min interval between injections to allow for complete equilibration. Each titration was continued until 4.5−6 equiv of M(II) had been added to ensure that no additional complexes were formed in excess titrant. A background titration, consisting of the identical titrant solution but only the buffer solution in the sample cell, was subtracted from each experimental titration to account for the heat of dilution. These data were analyzed with a two-site binding model by the Windows-based Origin software package supplied by MicroCal. The equilibrium binding constant, K_a, and the enthalpy change, ΔH, were used to calculate ΔG and ΔS using the Gibbs free energy relationship (eq 1)

$$\Delta G° = - RT \ln[K_a] = \Delta H° - T\Delta S° \qquad (1)$$

where $R = 1.9872$ cal mol^{-1} K^{-1}. The relationship between K_a and K_d is defined as

$$K_d = 1/K_a \qquad (2)$$

Individual ArgE solutions were prepared by diluting stock enzyme solutions in 25 mM Chelex 100 treated HEPES buffer (pH 7.6) containing 150 mM KCl.

Spectroscopic Measurements. Electronic absorption spectra were recorded on a Shimadzu UV-3101PC spectrophotometer, and all solutions were degassed prior to performing an experiment. Low-temperature EPR (electron paramagnetic resonance) spectroscopy was performed using a Bruker Elexsys E500 spectrometer equipped with an ER 4116 DM dual-mode X-band cavity and an Oxford Instruments ESR-900 helium flow cryostat. Background spectra recorded on a buffer sample were aligned with and subtracted from experimental spectra as described previously.[14,15] EPR spectra were recorded at microwave frequencies of 9.6330 ± 0.0005 GHz: precise microwave frequencies were recorded for individual spectra. All spectra were recorded at 12K, with 10.6 G magnetic field modulation at 100 kHz modulation frequency and 2 mW microwave power, conditions that were determined to be nonsaturating. Computer simulations of EPR spectra were carried out using Xsophe v.1.1.2 (Bruker Biospin GmbH, Rheinstetten, Germany).[16] Parameters were fit to the spin Hamiltonian

$$H = \beta \mathbf{gHS} + \mathbf{SDS} + \mathbf{SAI} \qquad (3)$$

where all of the variables have their standard meanings. Under this formalism $D > 0$ corresponds to an $M_S = |\pm 1/2\rangle$ ground state and $D < 0$ corresponds to an $M_S = |\pm 3/2\rangle$ ground state.

Results

Quaternary Protein Structure of ArgE and Metal Binding Properties. Denaturing gels of purified ArgE indicate a mass of ~42 000 Da per monomer. However, nondenaturing gels provided two bands at ~170 000 and ~340 000 Da (Figure 1). The more intense of the two migrates slightly slower than the 132 kDa dimeric form of bovine serum albumin, while the second band, which is very faint, migrates slightly slower than the 272 kDa trimeric form of urease. These data suggest the formation of an octamer (theoretical molecular weight = 340 kDa); however, the majority of ArgE assembles as a tetramer (molecular weight 170 kDa). Protein concentrations were determined using a theoretical ε_{280} value of 41 250 M^{-1} cm^{-1}, which differs slightly from the value $\varepsilon_{280} = 49 412$ M^{-1} cm^{-1} reported by Javid-Majd and Blanchard[11] and significantly from the $\varepsilon_{280} = 101 300$ M^{-1} cm^{-1} value reported by Meinnel et al.[10] The theoretical value of $\varepsilon_{280} =$

41 250 M^{-1} cm^{-1} represents a theoretical upper limit, according to the amino acid sequence, that would be expected without inhibition of absorbance by protein structure. Since denaturation of ArgE in 6 M guanidinium chloride shows no increase in absorbance at 280 nm, the ε_{280} value of 41 250 M^{-1} cm^{-1} was used. On the basis of this molar absorptivity the as-purified ArgE enzyme contained ~1 Zn(II) ion per monomer as determined via inductively coupled plasma-atomic emission spectrometry (ICP-AES).
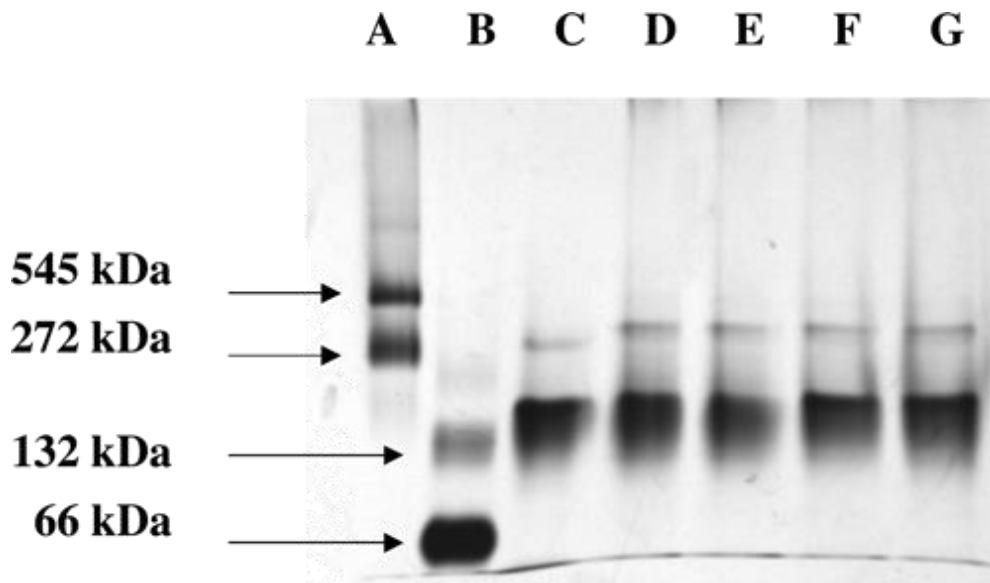

Figure 1 Native PAGE gel of ArgE. The two bands in lane A represent the 272 kDa trimeric and 545 kDa hexameric forms of urease, and the two bands in lane B represent the 66 kDa monomeric and 132 kDa dimeric forms of bovine serum albumin included as molecular weight standards purchased from Sigma. Lanes C−G each contain 8 μg of apo-ArgE that was incubated with varying concentrations of Zn(II). The ArgE in lane C contained no metal. It was dialyzed in 10 mM EDTA and then in 50 mM Chelex 100 treated HEPES, pH 7.5.

Zn(II)- and Co(II)-Loaded ArgE. Incubation of apo-ArgE with either Zn(II) or Co(II) provided ArgE enzymes with 100% and ~200% of the observed activity of the as purified enzyme. Titration of apo-ArgE with Zn(II) provided a plot of k_{cat} vs [Zn(II)] (Figure 2). For these studies a 10 μM enzyme concentration was used, and the enzyme was incubated at 25 °C for 20 min after each addition of Zn(II). The dissociation constant (K_d) of Zn(II) was determined by fitting the activity titration data (Figure 2) to eq 4

$$r = pC_s/(K_d + C_s) \qquad (4)$$

where p is the number of sites for which interaction with Zn(II) is governed by the intrinsic dissociation constant, K_d, and r is the binding function calculated by the conversion of the fractional saturation (f_a) using eq 5

$$r = f_a p \qquad (5)$$

C_S, the free metal concentration, was calculated using eq 6

$$C_S = C_{TS} - rC_A \qquad (6)$$

where C_{TS} and C_A are the total molar concentrations of metal and enzyme, respectively. The K_d value obtained by fitting these data via an iterative process that allowed both K_d and p to vary provided a p value of 1 and a K_d value of 6 μM (Figure 3).
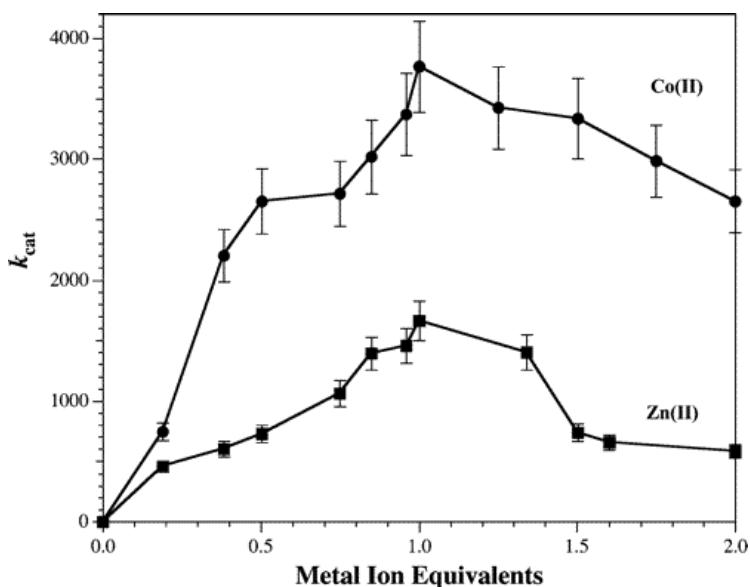

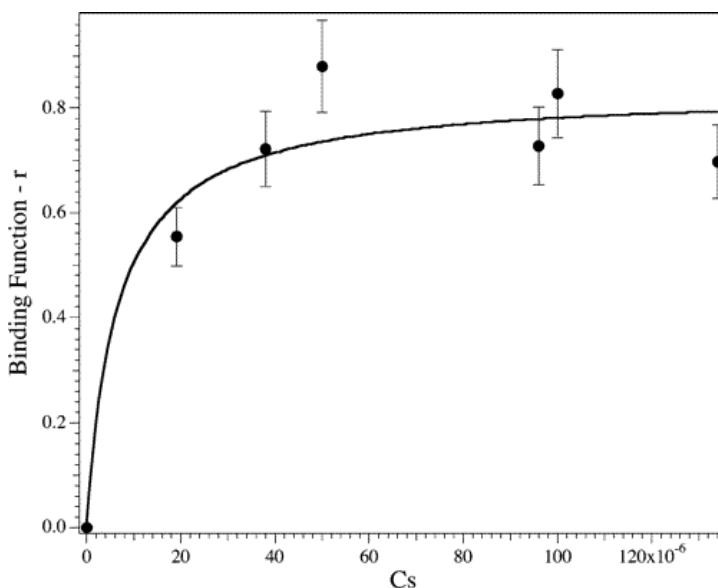**Figure 2** k_{cat} of a 10 μM apo-ArgE titrated with 0.2−2.0 equiv of Zn(II) or Co(II).

Figure 3 Plot of binding function r vs CS (the concentration of free metal ions in solution) for Zn(II) titration into apo-ArgE (50 mM KH_2PO_4, pH 7.5).

Isothermal Titration Calorimetry. ITC measurements were carried out on a MicroCal OMEGA ultrasensitive titration calorimeter at 25 ± 0.2 °C. Association constants (K_a) were obtained by fitting these data, after subtraction of the background heat of dilution, via an interactive process using the Origin software package. This software package uses a nonlinear least-squares algorithm, which allows the concentrations of the titrant and sample to be fit to the heat-flow-per-injection to an equilibrium binding equation for two noninteracting sites (Figure 4). The K_a value, enzyme-metal stoichiometry (n), and change in enthalpy ($\Delta H°$) were allowed to vary during the fitting process. For ArgE, K_d values determined for Zn(II) binding revealed one tight binding site with a K_d value of 2.7 µM while the second metal binding site exhibited weaker Zn(II) affinity with a K_d value of 51 µM. The energy change observed for the first Zn(II) binding event was exothermic, while the second metal binding site exhibited endothermic character (Table 2). Similar to Zn(II) binding, Co(II) binding to ArgE revealed a tight binding site (K_d = 0.4 µM) and a weak second metal binding site (K_d = 153 µM). The thermodynamic properties observed for Co(II) were similar to Zn(II) binding to ArgE in that the first metal binding event was endothermic while the second was exothermic (Table 2).
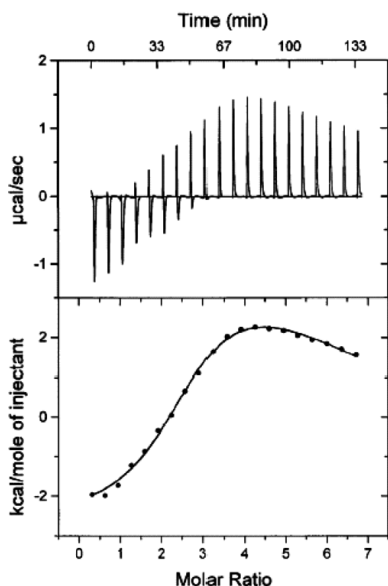
Figure 4 (A) ITC titration of a 70 µM solution of apo-ArgE with a 2.5 mM solution of Zn(II). (B) Fit of the ITC data for ArgE after subtraction of the heat of dilution. (Reaction conditions: 25 °C in 50 mM HEPES buffer, pH 7.5, and 150 mM KCl).

Table 1. Kinetic Constants for ArgE Incubated with 1 Equiv of Zn(II) or Co(II)

	k_{cat} (s^{-1})	K_m (mM)	K_{cat}/K_m (M^{-1} s^{-1})
[Zn(ArgE)]	1600	0.8	2.0×10^6
[Co(ArgE)]	3800	1.2	3.2×10^6

Table 2. Thermodynamic Parameters for the Hydrolysis of l-*p*NA by Zn(II)-Loaded AAP Compared to Those for the Hydrolysis of NAO by Zn(II)- or Co(II)-Loaded ArgE

	[ZnZn(AAP)]	[Zn(ArgE)]	[Co(ArgE)]
$\Delta G^{\ddagger}$ (kJ/mol)	62.1	54.8	51.5
$\Delta H^{\ddagger}$ (kJ mol)	34.0	23.2	31.8
$\Delta S^{\ddagger}$ (J/mol K)	−94.2	−106	−66.0
E_a (kJ/mol)	36.5	25.6	34.3

Temperature Dependence of ArgE-Catalyzed Hydrolysis of NAO. The thermal stability of ArgE was examined in 50 mM Chelex 100 treated phosphate buffer at pH 7.5. ArgE was not particularly thermally stable; therefore, the hydrolysis of NAO was only measured between 20 and 45 °C. In a simple rapid equilibrium $V_{max}/[E] = k_p$, the first-order rate constant. Since the enzyme concentration was not altered over the course of the experiment, an Arrhenius plot was

constructed by plotting ln k_{cat} vs $1/T$ (Figure 5). A linear plot was obtained, indicating that the rate-limiting step does not change as the temperature is increased.[17] From the slope of the line the activation energy, E_a, for temperatures between 293 and 328 K was calculated to be 25.6 ± 2 kJ/mol for [Zn·(ArgE)] (Table 2). Since the slope of an Arrhenius plot is equal to $-E_{a1}/R$, where $R = 8.3145$ J K^{-1} mol^{-1}, other thermodynamic parameters were calculated by the following relations: $\Delta G^{\ddagger} = -RT \ln(k_{cat}h/k_BT)$, $\Delta H^{\ddagger} = E_a - RT$, $\Delta S^{\ddagger} = (\Delta H^{\ddagger} - \Delta G^{\ddagger})/T$, where k_B, h, and R are the Boltzmann, Planck, and gas constants, respectively. The enthalpy and entropy of activation were calculated to be 23.2 ± 2 kJ/mol and −106.0 ± 9 J/(mol K), respectively. The free energy of activation at 25 °C was calculated to be 54.8 kJ/mol. An Arrhenius plot was also constructed for [Co·(ArgE)] (Figure 5), which provided an E_a value of 34.3 ± 3 kJ/mol. The remaining thermodynamic parameters are $\Delta G^{\ddagger} = 51.5$ kJ/mol, $\Delta H^{\ddagger} = 31.8 \pm 3$ kJ/mol, and $\Delta S^{\ddagger} = -66.0 \pm 6$ J/(mol K) (Table 2).
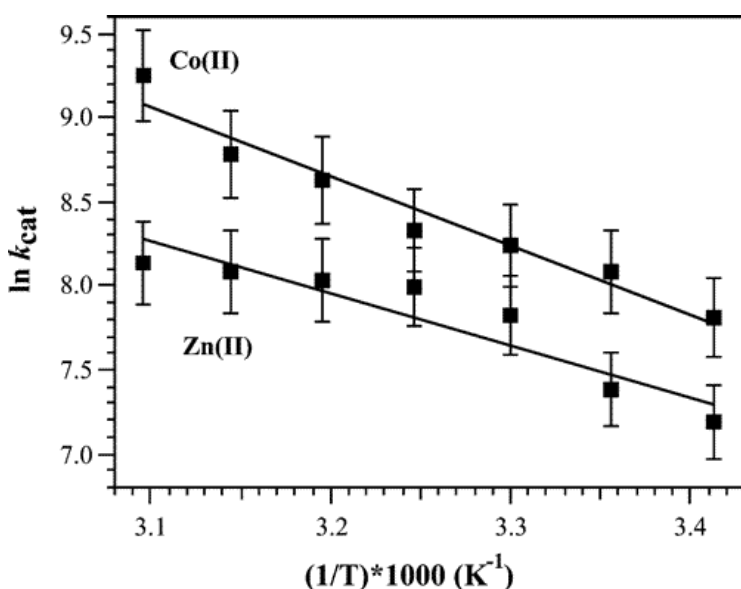

Figure 5 Arrhenius plot for NAO deacetylation catalyzed by ArgE loaded with 1 equiv of Zn(II) or Co(II).

Electronic Absorption Spectra of Co(II)-Loaded ArgE. The electronic absorption spectra of [Co·(ArgE)] and [CoCo(ArgE)] were recorded, and the absorption due to apo-ArgE was subtracted in both cases (Figure 6). The observed UV−vis spectrum for [Co·(ArgE)] exhibited three distinct peaks at 560, 619, and 705 nm with molar absorptivities (ε) of ε$_{560}$ = 114 M^{-1} cm^{-1}, ε$_{619}$ = 119 M^{-1} cm^{-1}, and ε$_{705}$ =

52 M^{-1} cm^{-1}. The addition of a second equivalent of Co(II) ([CoCo(ArgE)]) increased the intensity of each of the observed absorption bands, providing ε values of ε_{560} = 229 M^{-1} cm^{-1}, ε_{619} = 290 M^{-1} cm^{-1}, and ε_{705} = 121 M^{-1} cm^{-1} (Figure 6). These data suggest that both Co(II) binding sites in ArgE are five coordinate.
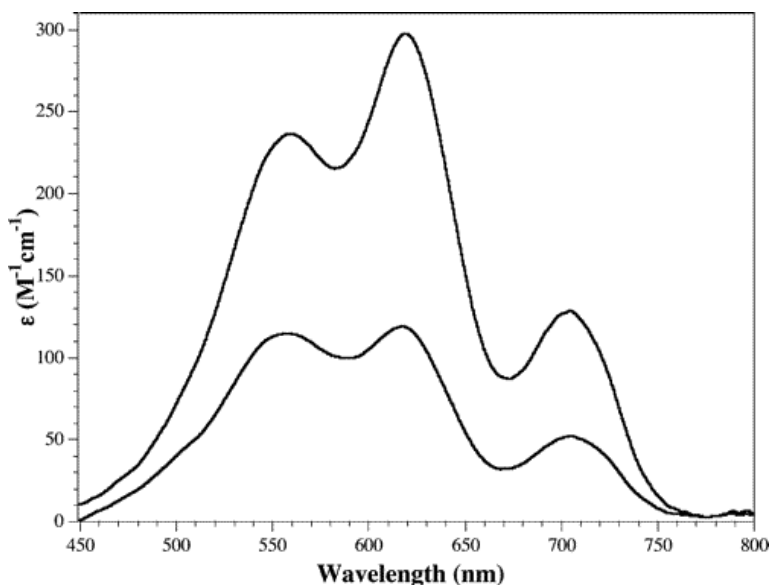

Figure 6 UV−vis absorption spectra of apo-ArgE titrated with 1 (lower) and 2 (upper) equiv Co(II) to form [Co·(ArgE)] and [CoCo(ArgE)], repectively. Spectra were recorded with 1 mM enzyme in HEPES buffer pH 7.5.

EPR Spectral Characterization of Co(II)-Loaded ArgE. The EPR spectra of Co(II)-loaded ArgE were recorded as a function of equivalents of added Co(II) (Figure 7). The spectra are complex and changed as subsequent quarter equivalents of Co(II) were added. To deconvolute the various species present in the EPR samples, difference spectra were generated (Figure 8) from which three basis spectra were extracted (traces 7C, 7E, and 7K). That these spectra corresponded to single chemical species is supported by computer simulation of the spectra (traces 7D, 7F, and 7L). Linear combinations of these simulations were then used to successfully simulate all the experimental spectra (Figure 7), and double integration of each of up to three components of the simulated spectra provided estimates for the spin concentration as a function of added Co(II) (Figure 9). Even at the lowest concentrations of added Co(II) two species were evident which we term the rhombic and axial signals. The rhombic signal was simulated (trace 7D) assuming S = 3/2, M_S = $|\pm1/2\rangle$, $g_\parallel$ = 2.475, $g_\perp$

= 2.250, D = 50 cm^{-1} (i.e., $\gg h\nu$), E/D = 0.25, A_y(^{59}Co) = 9.4 × 10^{-3} cm^{-1}. The axial signal was simulated assuming S = 3/2, M_S = $|\pm 1/2\rangle$, $g_\parallel$ = 2.300, $g_\perp$ = 2.275, D = 50 cm^{-1} (i.e., $\gg h\nu$), E/D = 0.08 and showed no evidence of ^{59}Co I = 7/2 hyperfine structure. A third species was only seen at Co(II) concentrations between 1 and 2 equiv; therefore, we term this signal the dicobalt signal. The dicobalt signal is similar to dinuclear Co(II)-loaded forms of other dinuclear metallohydrolases, notably the aminopeptidase from *Vibrio proteolyticus*[14,15] and the methionyl aminopeptidases from *E. coli* and *Pyrococcus furiosus*.[18,19] The dicobalt signal was simulated assuming S = 3/2, M_S = $|\pm 1/2\rangle$, $g_\parallel$ = 2.200, $g_\perp$ = 2.350, D = 50 cm^{-1} (i.e., $\gg h\nu$), E/D = 0.08. It is noteworthy that while the intensity of the dicobalt signal increases upon addition of more than 1 equiv Co(II), that of the rhombic signal, and the total spin concentration, decreases.
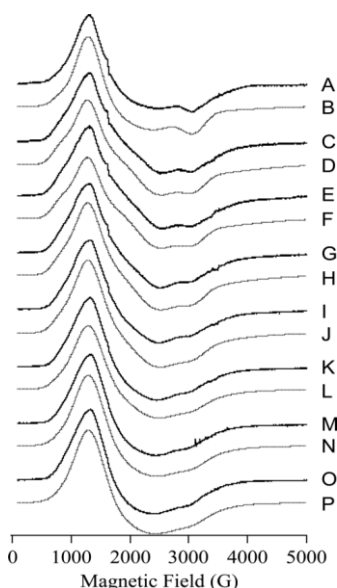

Figure 7 EPR spectra of ArgE were recorded after incubation with 0.21 (A), 0.42 (C), 0.63 (E), 0.84 (G), 1.05 (I), 1.26 (K), 1.47 (M), and 1.68 (O) equiv of Co(II). Traces B, D, F, H, J, L, N, and P are the corresponding computer simulations. The simulations were generated by adding various proportions of the simulated spectra presented in Figure 8, traces D, F, and L. The spin densities accounted for by each component for each of the simulated spectra are presented in Figure 9.
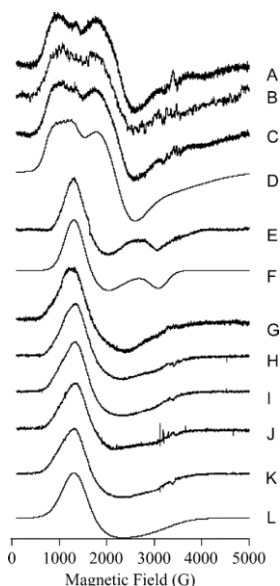
Figure 8 Paramagnetic species that contribute to EPR spectra of ArgE incubated with Co(II). Traces A, B, C, G, H, I, J, and K are difference spectra generated by subtraction of successive experimental spectra from Figure 7, where trace 8A = 7C − 7A, 8B = 7E − 7C, 8C = 7E − 7A, 8E = 7A − 8A, 8G = 7G − 7E, 8H = 7I − 7G, 8I = 7K − 7I, 8J = 7M − 7K, and 8K = 7O − 7M. Trace D is a theoretical spectrum assuming $S = 3/2$, $M_S = |\pm 1/2\rangle$, $g_\parallel = 2.475$, $g_\perp = 2.250$, $D = 50$ cm^{-1} (i.e., $\gg h\nu$), $E/D = 0.25$, $A_y(^{59}Co) = 9.4 \times 10^{-3}$ cm^{-1}. Trace F is a theoretical spectrum assuming $S = 3/2$, $M_S = |\pm 1/2\rangle$, $g_\parallel = 2.300$, $g_\perp = 2.275$, $D = 50$ cm^{-1} (i.e., $\gg h\nu$), $E/D = 0.08$. Trace L is a theoretical spectrum assuming $S = 3/2$, $M_S = |\pm 1/2\rangle$, $g_\parallel = 2.200$, $g_\perp = 2.350$, $D = 50$ cm^{-1} (i.e., $\gg h\nu$), $E/D = 0.08$.
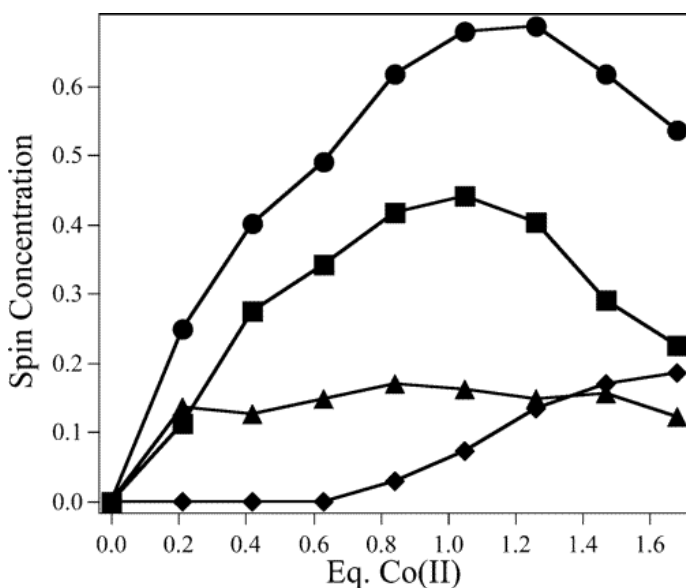

Figure 9 EPR spectrometric titration of ArgE with Co(II). The spin densities due to each of the species contributing to the EPR spectra of ArgE incubated with Co(II) are shown as a function of [Co(II)]. Trace A (solid circles) shows the total spin density.

Traces B (•), C (▲), and D (♦) show the spin densities due to the rhombic (Figure 7D), axial (Figure 7F), and dicobalt (Figure 7L) species.

Discussion

The emergence of several pathogenic bacterial strains that are resistant to all currently available antibiotics poses a tremendous worldwide health problem.[5-8] The arginine biosynthetic pathway offers several potential antibacterial targets that have yet to be explored.[10,11,20,21] ArgE, one of the members of this pathway, has been identified in several pathogenic bacteria such as *E. coli* O157:H7, *Salmonella typhimurium*, *Legionella pneumophila*, *Yersinia pseudotuberculosis*, *Bordetella pertussis, Vibrio cholerae*, *Staphylococcus aureus,* and *Mycobacterium tuberculosis*.[10,11,20,21] Alignment of each of these amino acid sequences with the structurally characterized dinuclear Zn(II) hydrolases AAP and CPG$_2$ revealed significant sequence homology, especially in the amino acids functioning as metal ligands.[11] However, it should be noted that no catalytically important amino acid residues have been identified for any ArgE enzyme. The enzymatic activity of the ArgE from *E. coli* was recently shown to be dependent on Zn(II) ions;[11] therefore, ArgEs were proposed to belong to the same peptidase family, M28, as AAP and CPG$_2$.[22] In an effort to gain insight into the structural and catalytic properties of the active site of ArgEs, we examined the metal binding properties via kinetic, thermodynamic, and spectroscopic methods for the Zn(II)- and Co(II)-loaded forms of the ArgE enzyme from *E. coli*.

ArgE was previously shown to be a homodimer;[11] however, electrophoretic analysis of ArgE using an 8% nondenaturing polyacrylamide gel indicates that the enzyme can also form a homotetramer and even a homooctamer. These data suggest that the oligamerization of ArgE may play a physiological regulatory role. Similar to AAP, it was shown that the as-purified ArgE enzyme contains only one tightly bound Zn(II) ion and exhibits ~90% of its total activity in the presence of one Zn(II) ion. The k_{cat} and K_m values for ArgE loaded with 1 equiv of Zn(II) ([Zn·(ArgE)]) were found to be 1600 s^{-1} and 0.8 mM, respectively, while [Co·(ArgE)] provided k_{cat} and K_m values of 3800 s^{-1} and 1.2 mM, respectively. These data are somewhat different from the previously reported values (k_{cat} = 290 s^{-1} and K_m = 7.2 mM for [ZnZn(ArgE)] and k_{cat} = 1100 s^{-1} and K_m = 1.3

mM for [CoCo(ArgE)]).[11] The difference is likely due to the fact that the original kinetic data was recorded with a large excess of divalent metal ions, which we found inhibits ArgEs ability to hydrolyze NAO, a phenomenon that is typical of metallohydrolases that contain dinuclear sites.[20,23,24] As is typical for many metallohydrolases, ArgE can be activated by a number of divalent metal ions including manganese.[25] These data are similar to those reported for the *dapE*-encoded *N*-succinyl-l,l-diaminopimelic acid desuccinylase (DapE), an enzyme involved in the *meso*-diaminopimelate (mDAP)/lysine biosynthetic pathway that shares a significant amount of sequence homology to ArgE.[26] Interestingly, AAP cannot be activated by Mn(II),[27] whereas the leucine aminopeptidase from bovine lens (bLAP) is active in the presence of Mg(II) or Mn(II).[28] The fact that ArgE is active with such a broad range of metals is likely indicative of its overall physiological importance within bacterial cells.

Titration of apo-ArgE with Zn(II) confirmed that the enzyme is ~90% active after the addition of only 1 equiv of Zn(II). Fits of these titration data provided a K_d value for the first metal binding site of 6 μM. Since only one metal ion is bound to the enzyme active site, these K_d values correspond to the microscopic binding constants for the binding of a single metal ion to ArgE. This K_d value is similar to K_d values obtained for several other hydrolytic enzymes that contain mixed histidine−carboxylate active sites. For example, the K_d values for the first metal binding sites of DapE and AAP are 140 and 1 nM, respectively,[26,29] clostridial aminopeptidase exhibits a K_d of 2 μM,[30] the clostridial AMPP has a reported K_d value of 7 μM,[30] and the β-lactamase from *Bacillus cereus* has a K_d value of 620 nM.[31] Verification of the observed K_d value for the first metal binding site of ArgE was obtained from ITC. ITC measurements of Zn(II) and Co(II) binding to ArgE provided K_d values of 2.7 and 0.4 μM for the first metal binding sites, respectively, and K_d values of 51 and 153 μM for the second metal binding site for Zn(II) and Co(II), respectively. These data suggest that under physiological conditions in the absence of substrate the second metal binding site may only be partially occupied. For both Zn(II) and Co(II) the first metal binding event is exothermic while the second is endothermic. Interestingly, the Gibbs free energy does not change significantly upon substitution of Zn(II) by Co(II) and is similar to that observed for AAP.[32] Similarly, the entropic factor (Δ*S*) remains

approximately the same for the first metal binding event despite a large decrease in K_d for Co(II) binding to ArgE. However, ΔS becomes negative for the second Co(II) binding event but remains slightly positive for the second Zn(II) binding site. These data suggest a decrease in order around the second metal binding site.

Since ArgE is relatively stable at 45 °C, activation parameters for the ES‡ complex were obtained by examining the hydrolysis of NAO as a function of temperature. Construction of an Arrhenius plot from the temperature dependence of ArgE activity indicates that the rate-limiting step does not change as a function of temperature.[17] The activation energy (E_a) for the ES‡ complex is 25.6 ± 2 kJ/mol for [Zn·(ArgE)] and 34.3 ± 3 kJ/mol for [Co·(ArgE)]. The observed activation energy is similar to the E_a reported for AAP (36.5 kJ/mol) and DapE (31 kJ/mol), which are similar to Pronase and both thermolysin and carboxypeptidase A.[33-35] The enthalpy of activation at 25 °C for [Zn·(ArgE)] and [Co·(ArgE)] is 23.2 ± 2 and 31.8 ± 3 kJ/mol, respectively, while the entropy of activation was found to be −106 ± 9 and −66 ± 6 J/mol K, respectively, at 25 °C. The positive enthalpy is indicative of a conformation change upon substrate binding, likely due to the energy of bond formation and breaking during nucleophilic attack on the scissile carbonyl carbon of the substrate. On the other hand, the large negative entropy values suggest that some of the molecular motions are lost upon ES‡ complex formation, possibly due to hydrogen-bond formation between catalytically important amino acids and the substrate. All of these factors contribute to the large positive free energy of activation.

To further examine the active site of ArgE, electronic absorption spectra of Co(II)-loaded ArgE (1 mM) were recorded. Upon addition of 1 equiv of Co(II) under anaerobic conditions, three resolvable d−d transitions at 560, 619, and 704 nm (ϵ = 114, 119, and 52 M^{-1} cm^{-1}, respectively) were observed. Ligand-field theory predicts that optical transitions of four-coordinate Co(II) complexes give rise to intense absorptions (ϵ > 300 M^{-1} cm^{-1}) in the higher wavelength region (625 ± 50 nm) due to a comparatively small ligand-field stabilization energy, while transitions of octahedral Co(II) complexes have very weak absorptions (ϵ < 30 M^{-1} cm^{-1}) at lower wavelengths (525 ± 50 nm). Five-coordinate Co(II) centers show intermediate features, i.e.,

moderate absorption intensities ($50 < \varepsilon < 250$ M^{-1} cm^{-1}) with several maxima between 525 and 625 nm.[36,37] On the basis of the molar absorptivities and d−d absorption maxima of [Co·(ArgE)] the first metal binding site is likely five coordinate. These data are similar to those reported for AAP and DapE.[14,15,26,38] Upon addition of a second equivalent of Co(II) to [Co·(ArgE)] the observed absorption bands do not shift but an increase in molar absorptivity of ~2 times is observed ($\varepsilon_{560} = 229$ M^{-1} cm^{-1}, $\varepsilon_{619} = 290$ M^{-1} cm^{-1}, and $\varepsilon_{705} = 121$ M^{-1} cm^{-1}). These data suggest that the second metal binding site is also five coordinate. Because the second Co(II) ion is weakly bound to ArgE, an equilibrium exists between free and bound Co(II). Therefore, the reported ε values for the second Co(II) binding event are likely underestimated. These data differ from those reported for the Co(II)-loaded AAP and DapE enzymes where the second metal binding site has been suggested to be octahedral.[14,15,26,38]

Taken with the optical data, the EPR spectrum of [Co·(ArgE)] supports the assignment of a five-coordinate environment for the first Co(II) binding site. The predominant signal observed from ArgE upon addition of 1 equiv Co(II) is the rhombic signal. This signal exhibits high rhombic distortion of the axial zero-field splitting, suggestive of a highly axially asymmetric ligand field. The rhombic signal also exhibits resolved ^{59}Co hyperfine structure, indicative of low strains in the spin Hamiltonian parameters, i.e., of a site with a low degree of conformational freedom. Taken together, these observations suggest a low symmetry site, likely five coordinate, with a geometry constrained by inflexible protein bound ligands, as may be expected for an enzyme catalytic site in an entatic state. A second signal, the axial signal, also appears at low Co(II) concentrations but does not increase in intensity beyond 0.2 equiv of added Co(II) and does not correlate with activity. While the origin of this signal is unclear, it is unlikely that it is related to the function of ArgE. As the amount of added Co(II) approaches 1 equiv, a second, broad signal, the dicobalt signal, appears and increases in intensity with further addition of Co(II); at the same time both the intensity of the rhombic signal and the total intensity of the spectrum decrease with added Co(II) (Figure 9). The increase in the dicobalt signal and concomitant decrease in the rhombic signal are indicative of the formation of a dinuclear center. The overall decrease in total intensity of the EPR signal indicates that the Co(II) ions in the

dinuclear center exhibit spin-exchange interaction, with $\mathbf{S}_1 \cdot \mathbf{J} \cdot \mathbf{S}_2 > \beta \mathbf{g} \cdot \mathbf{H} \cdot \mathbf{S}$.

The EPR behavior of ArgE bound by Co(II) ions is, in fact, very similar to that of AAP.[14] In AAP a rhombic signal that exhibits resolved [59]Co hyperfine structure is observed upon addition of 1 equiv Co(II) and is due to a five-coordinated Co(II) ion that has been proposed to function as the catalytic metal ion. Upon addition of a second Co(II) ion to AAP a broad axial signal, very similar to the dicobalt signal observed for ArgE, appears with the concomitant loss of the rhombic signal and overall loss of signal intensity due to spin coupling of the Co(II) ions.[14] It is likely, therefore, that the active site of ArgE is highly similar to that of AAP. Subtle differences do, however, exist; the rhombic signal in AAP is in a pH-dependent equilibrium with an axial signal, and the axial signal is favored at physiological pH, whereas the rhombic signal is favored at high pH.[14] In contrast, the rhombic signal observed for ArgE is favored at physiological pH. This may indicate that the active site nucleophile in the resting state of AAP is water whereas in ArgE it is a hydroxyl ion. Another difference is in the effect of the second metal ion on activity. In AAP the presence of a second metal ion results in a small increase in activity, whereas a second Co(II) in ArgE has very little measurable effect on activity. These data indicate that the coordination geometry of the second metal ion differs in AAP and ArgE; specifically, electronic absorption data suggest a five-coordinate Co(II) in ArgE whereas the metal ion is six coordinate in AAP.

In conclusion, the kinetic and thermodynamic data presented herein provide evidence that two Zn(II) ions can bind to ArgE with K_d values that differ by ~20 times. Moreover, ArgE is nearly fully active upon addition of one metal ion. Therefore, ArgE behaves similarly to AAP in that one metal ion is the catalytic metal ion while the second likely plays a structural role. The spectroscopic data presented herein provides the first structural glimpse at the active site metal ions of any ArgE enzyme. Electronic absorption and EPR spectra of [Co·(ArgE)] and [CoCo(ArgE)] indicate that both divalent metal binding sites are five coordinate. In addition, the EPR data show clear evidence of spin−spin coupling between the Co(II) ions in the active site but only after addition of a second equivalent of Co(II). Combination of the

data presented herein provides the first physical evidence that the ArgE from *E. coli* contains a dinuclear Zn(II) active site, similar to AAP and CPG_2 (Figure 10). This finding is critical for the future design and synthesis of small molecule inhibitors that will target ArgE enzymes.
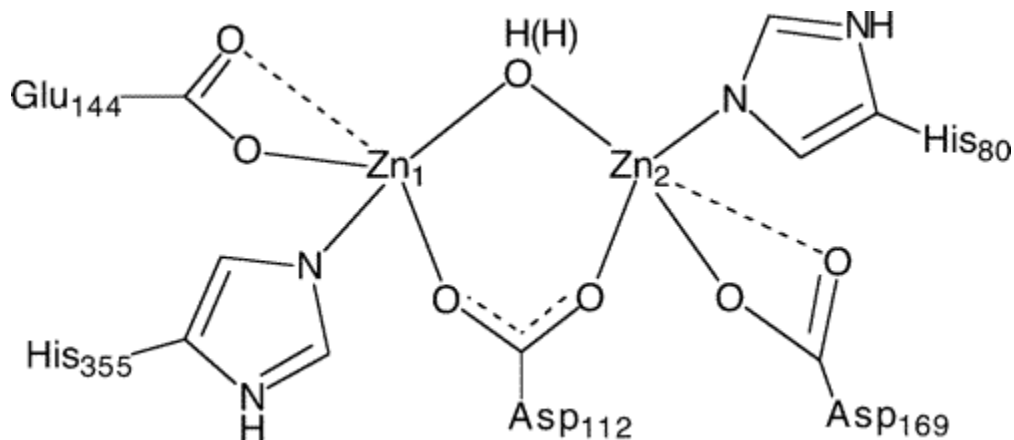

Figure 10 Proposed active site of the ArgE from *E. coli* based on sequence alignments with AAP and CPG_2.

Acknowledgment

References

[1]Leeb, M. *Nature* **2004**, *431*, 892−893.

[2]Walsh, C. *Nat. Rev. Microbiol.* **2003**, *1*, 65−70.

[3]Ecker, D.; Sampath, R.; Willett, P.; Wyatt, J.; Samant, V.; Massire, C.; Hall, T.; Hari, K.; McNeil, J.; Buchen-Osmond, C.; Budowle, B. *BMC Microbiol.* **2005**, *5*, 19−36.

[4]Henery, C. M. *Chem. Eng. News* **2000**, 41−58.

[5]Prevention, C. f. D. C. a. *MMWR Morb. Mortal. Wkly Rep.* **1995**, *44*, 1−13.

[6]Howe, R. A.; Bowker, K. E.; Walsh, T. R.; Feest, T. G.; MacGowan, A. P. *Lancet* **1997**, *351*, 601−602.

[7]Levy, S. B. *Sci. Am.* **1998**, *278*, 46−53.

[8]Chin, J. *New Scientist* **1996**, *152*, 32−35.

[9]Nemecek, S. *Sci. Am.* **1997**, *276*, 38−39.

[10]Meinnel, T.; Schmitt, E.; Mechulam, Y.; Blanquet, S. *J. Bacteriol.* **1992**, *174*, 2323−2331.

[11]Javid-Majd, F.; Blanchard, J. S. *Biochemistry* **2000**, *39*, 1285−1293.

[12]Chevrier, B.; Schalk, C.; D'Orchymont, H.; Rondeau, J.-M.; Moras, D.; Tarnus, C. *Structure* **1994**, *2*, 283−291.

[13]Rowsell, S.; Pauptit, R. A.; Tucker, A. D.; Melton, R. G.; Blow, D. M.; Brick, P. *Structure* **1997**, *5*, 337−347.

[14]Bennett, B.; Holz, R. C. *J. Am. Chem. Soc.* **1997**, *119*, 1923−1933.

[15]Bennett, B.; Holz, R. C. *Biochemistry* **1997**, *36*, 9837−9846.

[16]Griffin, M.; Muys, A.; Noble, C.; Wang, D.; Eldershaw, C.; Gates, K. E.; Burrage, K.; Hanson, G. R. *Mol. Phys. Rep.* **1999**, *26*, 60−84.

[17]Segel, I. H. *Enzyme Kinetics: Behavior and analysis of rapid equilibrium and steady-state enzyme systems*, 1st ed.; John Wiley & Sons: New York, 1975.

[18]D'souza, V. M.; Bennett, B.; Copik, A. J.; Holz, R. C. *Biochemistry* **2000**, *39*, 3817−3826.

[19]Copik, A. J.; Swierczek, S. I.; Lowther, W. T.; D'souza, V.; Matthews, B. W.; Holz, R. C. **2003**, *42*, 6283−6292.

[20]Holz, R. C.; Bzymek, K.; Swierczek, S. I. *Curr. Opin. Chem. Biol.* **2003**, *7*, 197−206.

[21]Girodeau, J.-M.; Agouridas, C.; Masson, M.; R., P.; LeGoffic, F. *J. Med. Chem.* **1986**, *29*, 1023−1030.

[22]*Handbook of proteolytic enzymes*; Barrett, A. J., Rawlings, N. D., Woessner, J. F., Eds.; Academic Press: London, 1998.

[23]Holz, R. C. *Coord. Chem. Rev* **2002**, *232*, 5−26.

[24]Lowther, W. T.; Matthews, B. W. *Chem. Rev.* **2002**, *102*, 4581−4607.

[25]Bennett, B.; W. A., A.; D'souza, V.; Ustynyuk, L.; Chen, G.; Holz, R. *J. Am. Chem. Soc.* **2002**, *124*, 13025−13034.

[26]Bienvenue, D. L.; Gilner, D. M.; Davis, R. S.; Bennett, B.; Holz, R. C. *Biochemistry* **2003**, *42*, 10756−10763.

[27]Prescott, J. M.; Wagner, F. W.; Holmquist, B.; Vallee, B. L. *Biochem. Biophys. Res. Commun.* **1983**, *114*, 646−652.

[28]Allen, M. P.; Yamada, A. H.; Carpenter, F. H. *Biochemistry* **1983**, *22*, 3778−3783.

[29]Prescott, J. M.; Wilkes, S. H. *Methods Enzymol.* **1976**, *45*, 530−543.

[30]Fleminger, G.; Yaron, A. *Biochim. Biophys. Acta* **1984**, *789*, 245−256.

[31]de Seny, D.; Heinz, U.; Wommer, S.; Kiefer, M.; Meyer-Klaucke; Galleni, M.; Frere, J.-M.; Bauer, R.; Adolph, H.-W. *J. Biol. Chem.* **2001**, *276*, 45065−45078.

[32]Bzymek, K. P.; Holz, R. C. *J. Biol. Chem.* **2004**, *279*, 31018−31025.

[33]Lumry, R.; Smith, E. L.; Glantz, R. R. *J. Am. Chem. Soc.* **1951**, *73*, 4330−4340.

[34]Kunugi, S.; Hirohara, H.; Ise, N. *Eur. J. Biochem.* **1982**, *124*, 157−163.

[35]Wu, C.-H.; Lin, W.-Y. *J. Inorg. Biochem.* **1995**, *57*, 79−89.

[36]Bertini, I.; Luchinat, C. *Adv. Inorg. Biochem.* **1984**, *6*, 71−111.

[37]Horrocks, W.; DeW., I., Jr.; Holmqust, B.; Thompson, J. S. *J. Inorg. Chem.* **1980**, *12*, 131−141.

[38]Prescott, J. M.; Wagner, F. W.; Holmquist, B.; Vallee, B. L. *Biochemistry* **1985**, *24*, 5350−5356.